

RESEARCH

Open Access



Negative Regulation of Cell Adhesion as a Driver of Brain Metastasis in NSCLC Patients with EGFR Amplification

Hainan Yang^{1,2†}, Congli Hu^{2†}, Yu Zhou^{3†}, Taoyuan Tong⁴, Luyao Qi¹, Weifang Yuan¹, Changguo Shan⁵, Weiping Hong⁵, Lei Wen^{6*}, Caicun Zhou^{2,7*} and Ming Lei^{1*}

Abstract

Brain metastases are strongly associated with a poor prognosis. Experimental animal models have provided valuable insights into the complex biology underlying brain metastasis, and translating these findings could pave the way for innovative management strategies for patients with brain metastases. Between May 2019 and June 2023, twenty-four lung cancer patients and thirty patients with brain metastases from lung cancer were enrolled at Guangdong Sanjiu Brain Hospital. Next-generation targeted panel sequencing (NGS) was performed on lung cancer tissue and surgical specimens from brain tumors for each patient. Brain metastasis mouse models were established through intracardiac injections, and the brain metastasis rate was analyzed. Our results showed that the rate of *EGFR* amplification was significantly higher in patients with brain metastases compared to lung cancer patients (40% vs. 12%). *EGFR*-overexpressing PC9 cell lines demonstrated significantly enhanced proliferation and infiltration abilities compared to their parental PC9 counterparts, as evidenced by CCK-8, wound healing, and transwell assays. Moreover, we observed a much higher brain metastasis rate in mice injected with *EGFR*-overexpressing PC9 cells compared to those injected with parental PC9 cells. RNA sequencing and Gene Ontology (GO) analysis revealed that differentially expressed genes were primarily associated with the “negative regulation of cell adhesion” in biological processes (BP) and “collagen-containing extracellular matrix” in cellular components (CC). This study identifies the negative regulation of cell adhesion as a key driver of brain metastasis in NSCLC patients with *EGFR* amplification.

Importance of the study

In comparing the sequencing results of brain metastatic tumor tissue and primary lung cancer tumor tissue, this study found that the detection rate of *EGFR* amplification was significantly higher in brain metastatic tumors than

[†]Hainan Yang, Congli Hu and Yu Zhou contributed equally to this work.

*Correspondence:

Lei Wen

wenlei1998@sina.com

Caicun Zhou

dr_caicunzhou@126.com

Ming Lei

leiming6891@163.com

Full list of author information is available at the end of the article



in lung cancer tissues. It is speculated that *EGFR* amplification may promote the development of brain tumors. Using lentiviral technology to establish cell lines overexpressing the *EGFR* gene, in vitro experiments showed that the proliferation and migration abilities of these cells were significantly enhanced. Furthermore, in vivo experiments confirmed that overexpression of the *EGFR* gene could promote the incidence of brain metastasis. These results suggest that targeted interventions against *EGFR* amplification in the future may reduce the incidence of brain metastasis.

Keywords Brain metastases, Non-small Cell Lung cancer, EGFR amplification, Genotyping, Cell adhesion

Introduction

Patients with brain metastases are often associated with a poor prognosis, combined with a high incidence rate, which has attracted widespread attention from scholars. Population-based research collected clinical data from patients with primary lung, melanoma, breast, renal, or colorectal cancer from 1973 to 2001 to calculate the incidence rate of brain metastases and draw the conclusion that the total incidence proportions of brain metastases was 9.6% for all primary sites combined, and patients with lung cancer accounting for the highest rate of 19.9% [1]. Evidence from prior research indicated that there was an increasing frequency of brain metastases with increasing tumor grade of patients within non-small cell lung cancer [2], other study showed that for lung cancer patients with metastases disease, the proportion of brain metastases is almost the same between small cell and non-small cell lung cancer presenting 23.5% and 15–26%, respectively [3].

Treatment options for patients with brain metastases typically include surgical removal, radiation therapy, and chemotherapy, and other treatment alternatives include targeted therapy, and immunotherapy [4]. However, patients with brain metastases appear to be refractory to all current treatments, leading to a continuous decline in quality of life. Whole-brain radiation therapy (WBRT) prolongs median survival from 1 to 3–6 months. The one-year survival rate for lung cancer patients with BM treated with whole-brain radiation therapy (WBRT) is approximately 10–20% and surgical resection or radio-surgery (RS) combined with adjuvant WBRT prolongs survival to approximately 8–11 months [5]. The adverse prognosis has presented novel challenges and also addresses increased research efforts to better understand the underlying mechanism of brain metastasis.

In this research, we conducted a comparative analysis of the NGS results between the lung and brain metastases tumor issue and further validated our hypothesis through in vitro experiments and subsequent in vivo animal studies.

Patients and Methods

Patient Population

Between May 2019 and June 2023, twenty-four patients with lung cancer and thirty patients with brain

metastases from lung cancer were enrolled at Guangdong Sanjiu Brain Hospital. Next-generation targeted panel sequencing (NGS) was performed on lung cancer tissue and surgical specimens of brain tumors for each patient.

Cell Culture

The parental PC-9 cells (EGFR exon 19 E746–A750 deletion) were obtained from the Cell Bank/Stem Cell Bank, Chinese Academy of Sciences. These cells were then transfected to express green fluorescence and luciferase, enabling fluorescence quantification and bioluminescence tracking. The signal intensity was measured using the Bright-Glo Luciferase Assay System (Promega). Cells were grown in DMEM supplemented with 10% fetal bovine serum, 1% penicillin-streptomycin, and 10 $\mu\text{L}/\text{mL}$ of corresponding antibiotics to ensure selection of transduced cells. Cells were kept at 37 °C and 5% CO₂. All cells used for in vivo and in vitro experiments were between passages 1–10.

Lentivirus Transduction

Luciferase lentivirus (pcSLenti-EF1-Luc2-P2A-BSR-CMV-MCS-WPRE) and EGFR-overexpressing lentivirus (pcSLenti-EF1-EGFP-P2A-Puro-CMV-EGFR-3xFLAG-WPRE) were purchased from OBiO Technology (Shanghai, China).

The procedure was as follows: (1) On Day 0, cells were plated in 10 cm dishes and allowed to adhere to the plate overnight. (2) On Day 1, the media was aspirated from the cell plates and replaced with fresh DMEM. The concentrated lentivirus was quickly thawed in a 37 °C water bath and immediately placed on ice. The virus was added to the cells dropwise, with the volume determined based on viral titration, and the plates were incubated overnight at 37 °C. (3) On Day 2, the lentiviral media was aspirated from the plates and replaced with fresh DMEM supplemented with 10% FBS. Cell selection started on Day 3. (4) To isolate clones stably expressing EGFR, the media was aspirated again and replaced with fresh DMEM supplemented with puromycin for selection.

Western Blot

The experimental procedure was performed as follows: (1) Cells were lysed on ice using RIPA buffer (YAMI, Shanghai, China) containing protease inhibitors. The

lysates were then mixed with loading buffer and denatured at 100 °C for 10 min. (2) Protein concentration was determined using the Bicinchoninic Acid (BCA) assay, after which the samples were subjected to SDS-PAGE (sodium dodecyl sulfate - polyacrylamide gel electrophoresis, SDS-PAGE). (3) The proteins were then transferred to polyvinylidene difluoride (PVDF) membranes (Millipore, Billerica, MA, USA). Prior to transfer, the PVDF membranes were activated by soaking them in methanol. (4) The membranes were incubated overnight at 4 °C with primary antibodies: EGFR (Abcam, 1:3000) and GAPDH (Affinity, 1:1000). (5) The following day, the membranes were incubated with the appropriate secondary antibody conjugated to horseradish peroxidase (HRP; anti-rabbit IgG, CST, 1:5000) at room temperature for 2 h. (6) After incubation, the membranes were washed three times with TBST (Tris-Borate-Sodium Tween-20 buffer), with each wash lasting 15 min. (7) Finally, the immunoreactive bands were visualized using Image Lab software after the addition of a luminol-based chemiluminescent substrate (ECL; Millipore).

CCK-8 Assay

The CCK-8 kit (Dojindo, Shanghai, China) was used to measure the proliferation of PC9 cells, which overexpress the EGFR gene, and parental PC9 cells. The procedure was as follows: (1) A total of 1000 cells in 100 μ L of medium per well were cultured in five replicate wells of a 96-well plate containing medium with 10% FBS. A concentration gradient was established using serial dilution, and different groups were set up (control group and *EGFR*-overexpressing group). (2) The 96-well plate was incubated in a cell culture incubator at 37 °C with 5% CO₂ for 24 h, allowing the cells to reach the logarithmic growth phase. (3) CCK-8 reagent (10 μ L) was added to 90 μ L of DMEM to prepare a working solution, and 100 μ L of this solution was added to each well. The plate was then incubated for 30 min. (4) After incubation, the optical density (OD) of each well was measured at a wavelength of 450 nm using a microplate reader. (5) The blank wells (without cells or CCK-8 reagent) were used as a control, with their OD values considered as background signal and subtracted from the experimental values.

Wound Healing Assay

Cells in the logarithmic growth phase were plated in a six-well plate at a density of 5×10^5 cells per well. Two experimental groups were established: one group consisting of PC9 cells that overexpress the EGFR gene, and the other group consisting of parental PC9 cells. The procedure was as follows: (1) A uniform scratch was made on the cell monolayer using a scratcher, with a scratch width of 300–500 μ m, ensuring the scratch was straight and covered the center of the well. (2) After scratching,

the wells were washed with PBS and then cultured in an incubator at 37 °C with 5% CO₂. (3) Photographs were taken at 0 h and 24 h under a microscope, and the experiment was repeated three times.

Transwell Migration Assay

The procedure was as follows: (1) The PC9 cells that overexpress the EGFR gene and the parental PC9 cells were diluted to a concentration of 10×10^4 cells/mL in serum-free DMEM medium. (2) A 200 μ L aliquot of the cell suspension was added to the upper chamber (top well) with serum-free DMEM medium, and 500 μ L of the cell suspension was added to the lower chamber (bottom well) with DMEM medium containing 20% fetal bovine serum. (3) The upper chamber was carefully immersed into the lower chamber liquid using sterile forceps. The 24-well plate containing the transwell inserts was then placed in the incubator (typically at 37 °C with 5% CO₂) for 24 h. (4) After incubation, the cell suspension was removed from the upper chamber, and the chamber was washed three times with PBS. (5) Fixative (4% paraformaldehyde) was added to the lower chamber to fix the cells, typically for 15 min. After fixation, the chamber was washed three times with PBS. (6) The cells were stained with crystal violet for 15 min. After staining, the upper chamber was observed under a microscope and photographed. Each experiment was repeated three times.

Animals and Brain Tumor Model Development

The tumor cells were subcutaneously inoculated into experimental mice, and fluorescence intensity as well as mouse body weight were measured weekly to assess tumor growth and plot growth curves. Mice were anesthetized using 2% isoflurane. After placement into a stereotactic device, approximately 150,000 PC-9 cells in 100 μ L of PBS were injected into the left cardiac ventricle, with a similar process in previous research [6, 7]. Bioluminescence signals and body weight were measured weekly to evaluate the growth of the tumor and verify the presence of metastases in the brain. In vivo metastasis experiments were conducted to examine the impact of selected PC9 cells overexpressing *EGFR*. Luciferase reporters were employed to track and determine the existence of brain metastases.

RNA Sequencing Was Performed on PC9 Cells that Overexpress the EGFR Gene and Parental PC9 Cells

The sequencing process involves the following steps: (1) total RNA was extracted from the tissue using TRIzol® Reagent according to the manufacturer's instructions. (2) RNA purification, reverse transcription, library construction and sequencing were performed at Shanghai Majorbio Bio-pharm Biotechnology Co., Ltd. (Shanghai, China) according to the manufacturer's instructions

(Illumina, San Diego, CA). (3) the raw paired end reads were trimmed and quality controlled by fastp with default parameters. Then clean reads were separately aligned to reference genome with orientation mode using HISAT2 software. (4) differential expression analysis and functional enrichment. To identify DEGs (differential expression genes) between two different samples, the expression level of each transcript was calculated according to the transcripts per million reads (TPM) method. In addition, functional-enrichment analysis including GO was performed to identify which DEGs were significantly enriched in GO terms and metabolic pathways at Bonferroni-corrected $P < 0.05$ compared with the whole-transcriptome background.

Statistical Analysis

Student's t-test and one-way ANOVA followed by a Fisher's LSD test were applied to determine the difference in the results of cell proliferation and viabilities. On survival endpoints, mice were sacrificed and the date of death was recorded. Kaplan-Meier curves were generated and compared using log-rank statistics. Significance for all tests was defined as $p < 0.05$. Statistical analysis was performed on GraphPad Prism software, SPSS and R statistical software (version 4.2.1).

Results

The Flowchart of this Study and Also the Basic Characteristic between Lung Cancer Patients and Patients with BM

Our main purpose was to identify the differences between lung cancer tissue specimens and brain metastasis tumor specimens and try to explore the mechanisms underlying the occurrence of brain metastasis (Fig. 1). This research enrolled 30 lung cancer patients with brain metastases. The median age was 55.5 (ranging from 37 to 76 years), and 53% (16/30) of the patients were female in this study. *EGFR* mutation accounts for the majority of patients in this study presenting 43% (13/30), including *EGFR* L858R, *EGFR* 19del, *EGFR* L861Q, *EGFR* G719A, *EGFR* G719S accounting for 13% (4/30), 17% (5/30), 7% (2/30), 3% (1/30), and 3% (1/30), respectively. In addition, all patients enrolled in this research had surgically removed brain tissue and were further verify by pathology (Table 1).

In Lung Adenocarcinoma, the Presence of *EGFR* Amplification Indicates a Poorer Prognosis

Survival data were downloaded from the public UCSC database (<https://xenabrowser.net/datapages>) and subjected to Kaplan-Meier survival analysis.

The results indicate that patients with *EGFR* amplification tend to have a poorer prognosis than those without *EGFR* amplification, with a statistically significant

difference (Fig. 2; HR: 0.61, 95% CI: 0.350–1.064, $P = 0.031$).

The Distribution of the Mutation Genes in the Lung and Brain Metastases Tissues

TP53 mutation was the most frequent mutation in brain metastases tissues presenting 60%. The rate of *EGFR* amplification was closely followed by and was much higher in patients with brain metastases compared to lung cancer patients (40% vs. 12%). Gene signatures, such as *LRP1B*, *RNF43*, and *MYC* were also commonly detected with the same percentage of 17%. Other mutation genes, including *EPAH3*, *CCND1*, *FGF4*, *CSMD3*, *CDKN2A*, and *PMS2* were also frequently seen, showing the same percentage of 13% (Fig. 3A).

The driver of *EGFR* account for the majority (67%, 16/24) of the mutation in lung cancer tissue, with *EGFR* L8585R, *EGFR* 19del and *EGFR* L861Q presenting 25%, 38%, and 4%, respectively. Without the driver genes, *TP53* was the most mutation gene in the lung cancer tissue with a mutation rate of 75%, and *APC* also has the higher mutation rate in the lung cancer tissue with a mutation rate of 21%, gene signature, such as *PMS2* and *CDK4* has the same rate of 17% in lung cancer tissues (Fig. 3B).

EGFR Overexpression Was Confirmed by Western Blot

The parental PC-9 cells (*EGFR* exon19 E746–A750 deletion) was transfected by *EGFR*-overexpressing lentivirus (pcSLenti-EF1-EGFP-P2A-Puro-CMV-EGFR-3xFLAG-WPRE) to display green color and overexpression of *EGFR* protein was further confirmed by western blot (Fig. 4).

Overexpression of *EGFR* Protein Enhanced the Proliferation and Migration Ability of NSCLC Cell Lines in Vitro

We assessed the proliferation and migration capabilities of NSCLC cell lines PC9 in vitro CCK8 assay, wound healing, and transwell assays. Our findings indicate that *EGFR* overexpression led to increased proliferation in CCK8 (Fig. 5A) and this trend was also evident in wound healing (Fig. 5B) and transwell assays (Fig. 5C).

Lentivirus Transduction of PC9 Cells Can Successfully Grow Tumor Subcutaneously

Tumor cells were injected subcutaneously into mice for the experiment, and fluorescence intensity was measured weekly, along with monitoring the mice's body weight, to evaluate tumor growth and create growth curves (Supplementary Data Fig. 1). Mice were sacrificed and the date of death was recorded, the subcutaneous tumor was removed and subjected to hematoxylin and eosin (HE) staining for further identification of tumor cells (Supplementary Data Figs. 2 and 3).

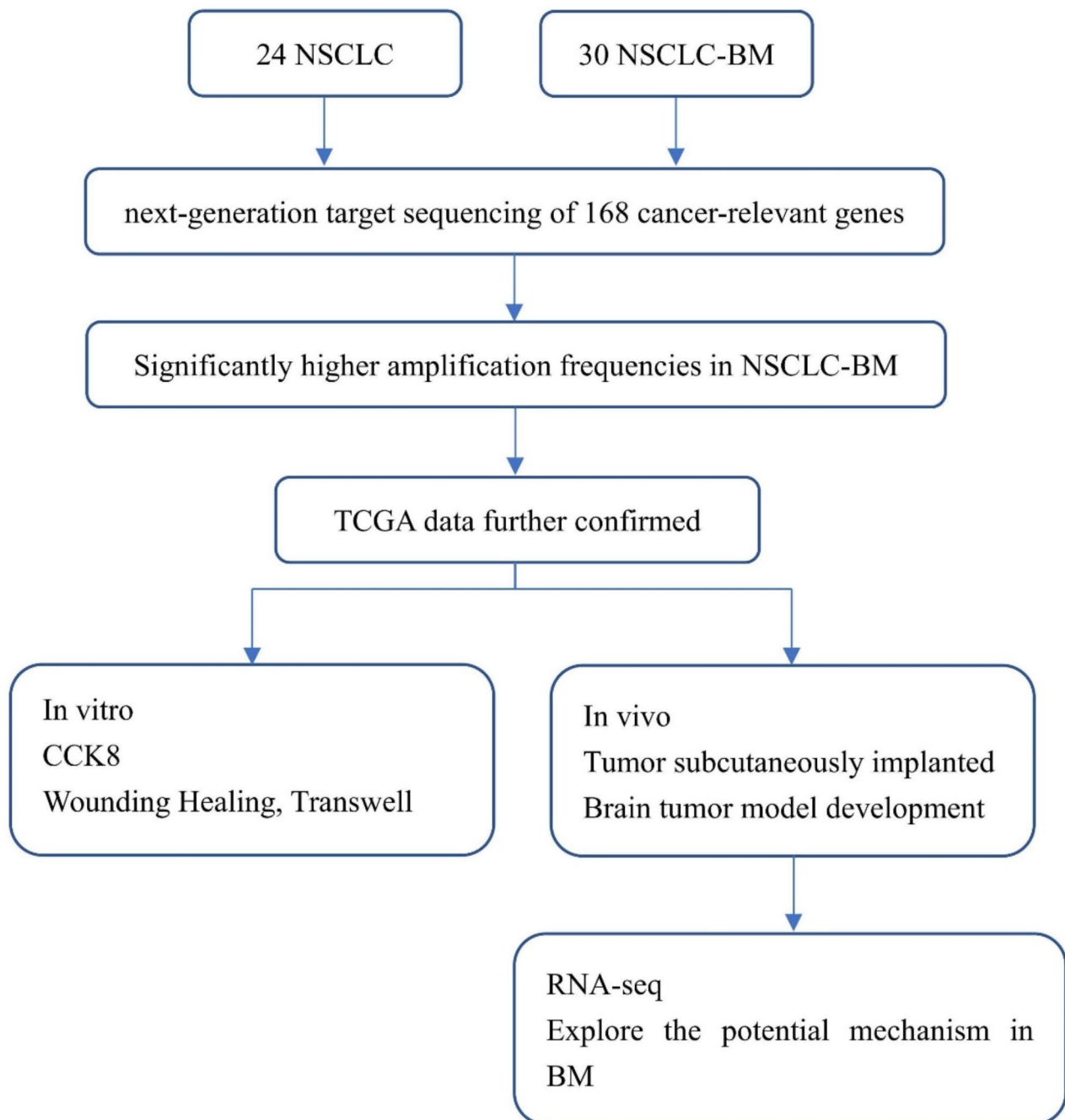


Fig. 1 Flowchart of this study design. Abbreviation: NSCLC, non-small cell lung cancer; NSCLC-BM, NSCLC patients with brain metastases

Table 1 The basic character of the patients in this study cohort

Characteristic	Cohort one n (%)	Cohort two n (%)
Tissue type	Brain Metastases	Lung Cancer
Number	30	24
Age (year)		
Median	55.5	59
Range	37–76	45–72
Gender		
Female	16 (53)	11 (46)
Male	14 (47)	13 (54)
Driver oncogene		
EGFR	13	16
L858R	4 (13)	6 (25)
T9del	5 (17)	9 (38)
L861Q	2 (7)	1 (4)
G719A	1 (3)	
G719S	1 (3)	
KRAS	5 (17)	3 (12)
ALK	3 (10)	
RET	1 (3)	
BRAF	1 (3)	
Wild Type	4 (13)	5 (20)
Diagnose of BM/lung cancer		
Pathology	30 (100)	24 (100)
Histologic type		
Adenocarcinoma	26 (87)	21 (87)
Squamous	4 (13)	3 (13)

Overexpression of EGFR Protein Enhanced the Brain Metastases Rate Compared To the Control Group

The mice were randomly assigned to control and experimental groups. In the control group, approximately 150,000 parental PC9 cells suspended in 100 μ L of PBS were injected into the left cardiac ventricle. In the *EGFR* amplification group, approximately 150,000 PC9 cells overexpressing the *EGFR* gene in 100 μ L of PBS were injected into the same site. After injection, the mice were marked with ear tags for accurate group identification. Luciferase reporters were used to monitor brain metastases, with bioluminescence signals measured weekly. The operator performing IVIS (In Vivo Imaging System) imaging was blinded to group assignments, ensuring the study was conducted in a blinded manner to minimize bias and maintain result integrity.

The mice were anesthetized with 2% isoflurane and positioned in a stereotactic device before intracardiac injection. Weekly assessments of bioluminescence signals and body weight were conducted to evaluate tumor growth and confirm brain metastases. Our results demonstrated that mice injected with *EGFR*-overexpressing PC9 cells exhibited a significantly higher rate of brain metastases compared to those injected with parental PC9 cells ($P < 0.05$) (Fig. 6).

RNA Sequencing Results of EGFR Overexpression in The PC-9 Cell Line Vs. The Parental PC-9 Cell Line

The heatmap of gene expression revealed that the samples were classified into two groups: control and *EGFR* amplification. The results showed that genes with significantly higher expression included *H2AX*, *TERT*, *HSD17B10*, *CITED4*, *COL13A1*, *NOMO3*, *NCEH1*, *SOCS2*, *LGALS1*, and *ANKRD29*. Genes with significantly lower expression included *TINCR*, *CYP4F12*, *PGLYRP3*, *CYP4F3*, *KRT16*, *BCAS1*, *KDM7A*, *TLE2*, *CD82*, and *ACKR3*. To explore the potential biological functions of the differentially expressed genes (DEGs), we performed Gene Ontology (GO) enrichment analyses, focusing on biological processes (BP), cellular components (CC), and molecular functions (MF). The results showed that DEGs in BP were significantly enriched in epidermis development, skin development, and the negative regulation of cell adhesion. For cellular components, DEGs were mainly enriched in collagen-containing extracellular matrix, apical plasma membrane, and endoplasmic reticulum lumen (Fig. 7).

Discussion

Upon diagnosis, cancer patients with metastases to the brain continue to experience a poor prognosis, characterized by increased morbidity, mortality, and a substantial rise in the cost during their treatment [8, 9]. The incidence of brain metastases continues to increase over time. The cumulative incidence after 5 years was estimated at 16.3% in patients with lung carcinoma [10]. The poor prognosis of lung cancer patients with brain metastases has led to increased focus in this area.

To figure out the different mutation genes between lung cancer and brain metastases tissue, our research

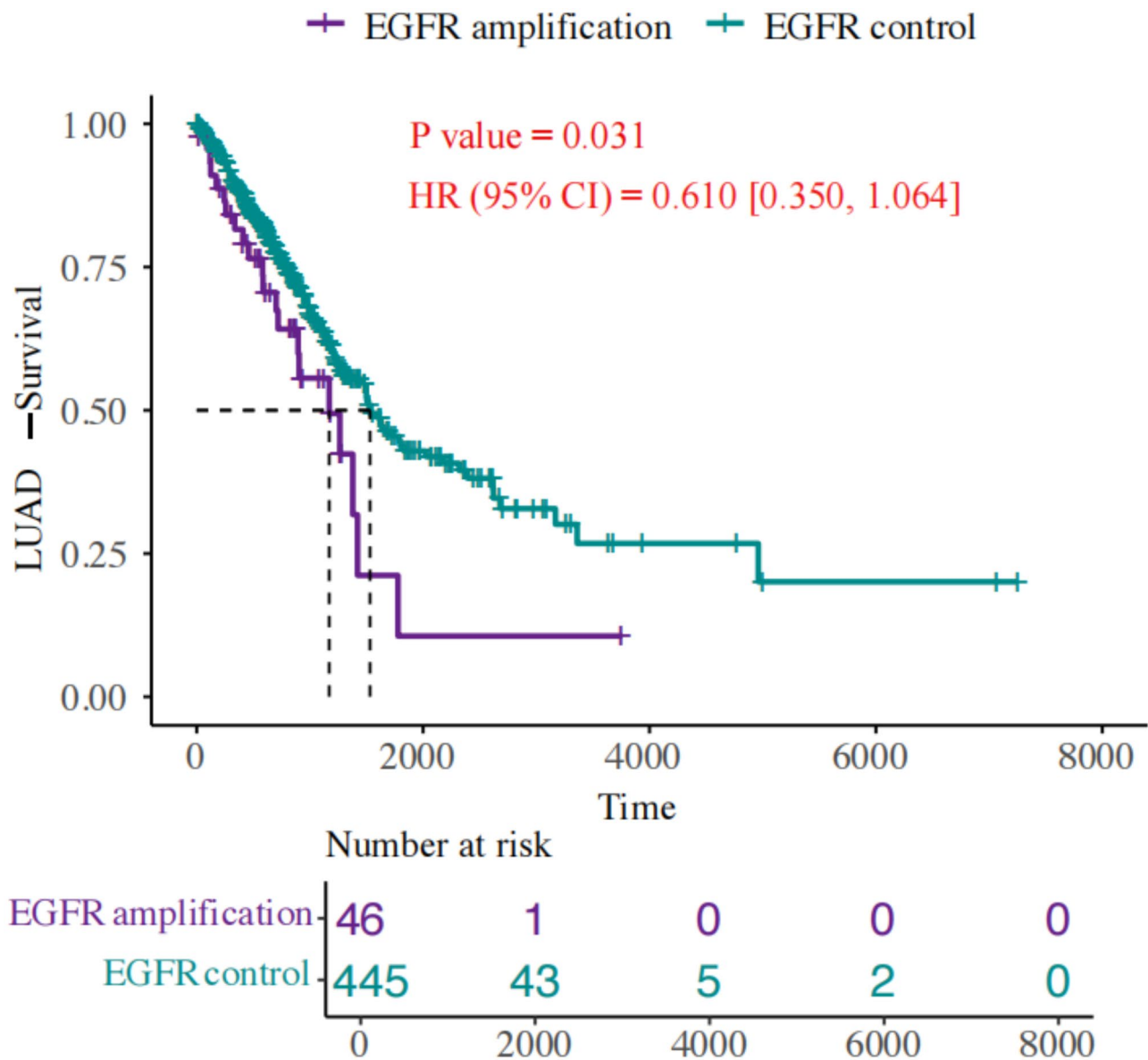


Fig. 2 Kaplan-Meier curves for overall survival of lung adenocarcinoma patients with or without EGFR amplification

compares the NGS results between lung cancer tissues and brain metastases samples trying to figure out the difference. Results demonstrated that the mutation rate of *EGFR* amplification was much higher in brain metastases tissue compared to the lung cancer samples (40% vs. 12%). In vitro experiments, we observed that compared to the control group, the *EGFR* gene

overexpression group exhibited significantly enhanced cell proliferation in CCK-8 assays and greater migration ability in wound healing and transwell experiments. Based on the promising results from our in vitro experiments, we proceeded to conduct in vivo experiments. Firstly, subcutaneous tumor formation experiments were performed by subcutaneously implanting PC9 cells which

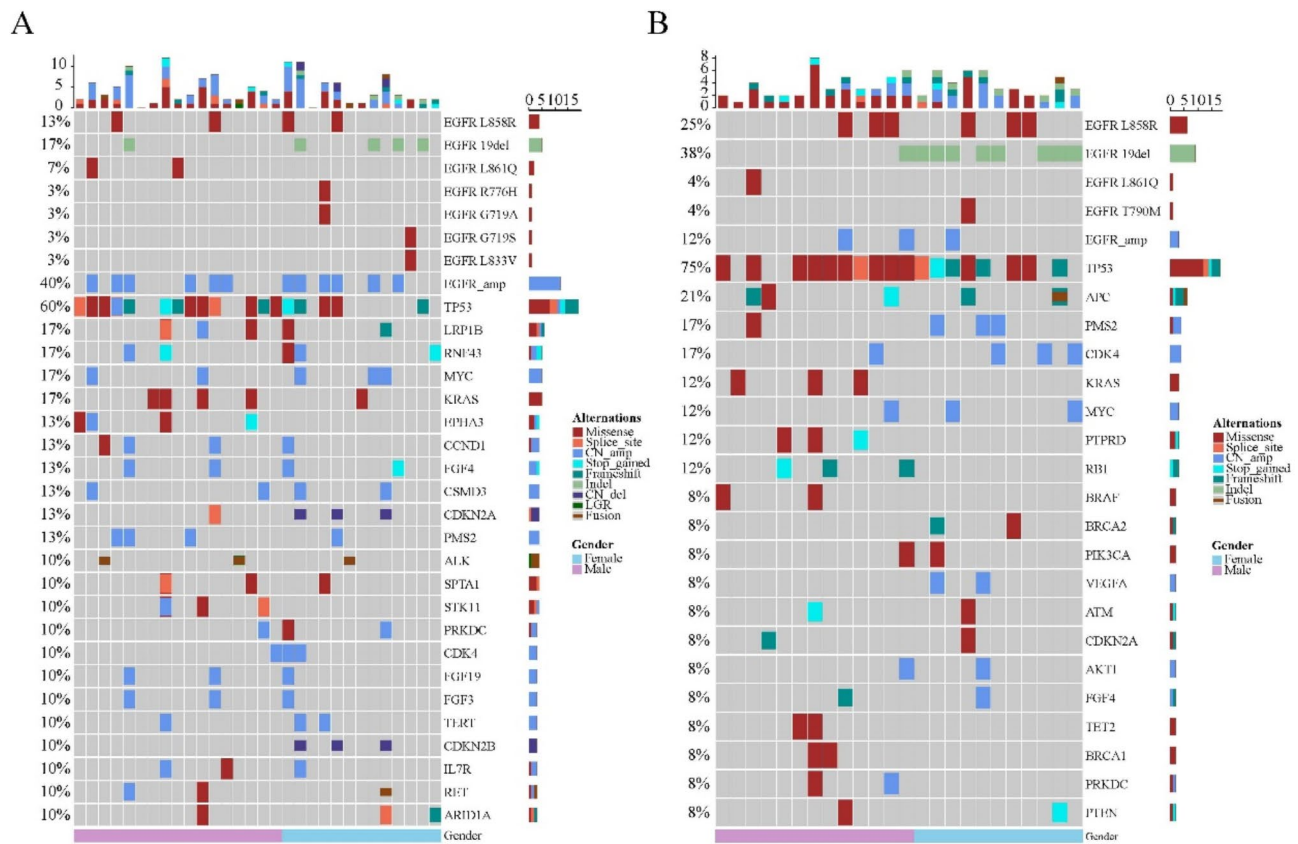


Fig. 3 Shows the oncoprint displaying the distribution of mutated genes in brain metastases tissue (A) and lung cancer tissue (B)

were overexpressing the *EGFR* gene into experimental mice. Weighed and tumor volume of the experimental mice were measured every 7 days, and results indicated that the tumors were well-established in the subcutaneous (Supplementary Data Fig. 1). Evidence from previous research suggests that *EGFR* gene overexpression is often associated with poor prognosis [11–14]. Further studies have identified *TP53* mutation and *EGFR* amplification as independent risk factors for recurrence-free survival (RFS) in resected *EGFR*-mutant lung adenocarcinoma [15]. To further confirm the function of *EGFR* overexpression in lung cancer patients with brain metastases, an animal model of brain metastases was built. And results from our study found that the brain metastases rate was much higher in the *EGFR* amplification group compared to the control group ($P < 0.05$).

RNA sequencing analysis comparing *EGFR*-overexpressing PC-9 cells with parental PC-9 cells revealed that DEGs in biological processes were significantly

enriched in pathways related to the negative regulation of cell adhesion. Through a series of literature reviews, we identified that *LGALS1* is associated with poor prognosis across various tumor types. For instance, a previous study on relapsed and refractory multiple myeloma (RRMM) analyzed differentially expressed genes in CD138⁺ plasma cells (PCs) at various disease stages and found a significant upregulation of *LGALS1* in proliferating stem-like plasma cells (PSPCs). Furthermore, survival analysis indicated that *LGALS1* is linked to unfavorable prognostic outcomes in multiple myeloma [16]. A similar study utilized RNA sequencing and identified galectin-1, encoded by *LGALS1*, as a critical factor contributing to resistance in the treatment of esophageal squamous cell carcinoma (ESCC) [17]. Additionally, another study demonstrated that *Lgals1* was overexpressed in the interstitial kidney of chronic kidney disease (CKD) mice. Treatment with Nobiletin (NOB) significantly reduced *Lgals1* expression while inhibiting PI3K and AKT phosphorylation [18].

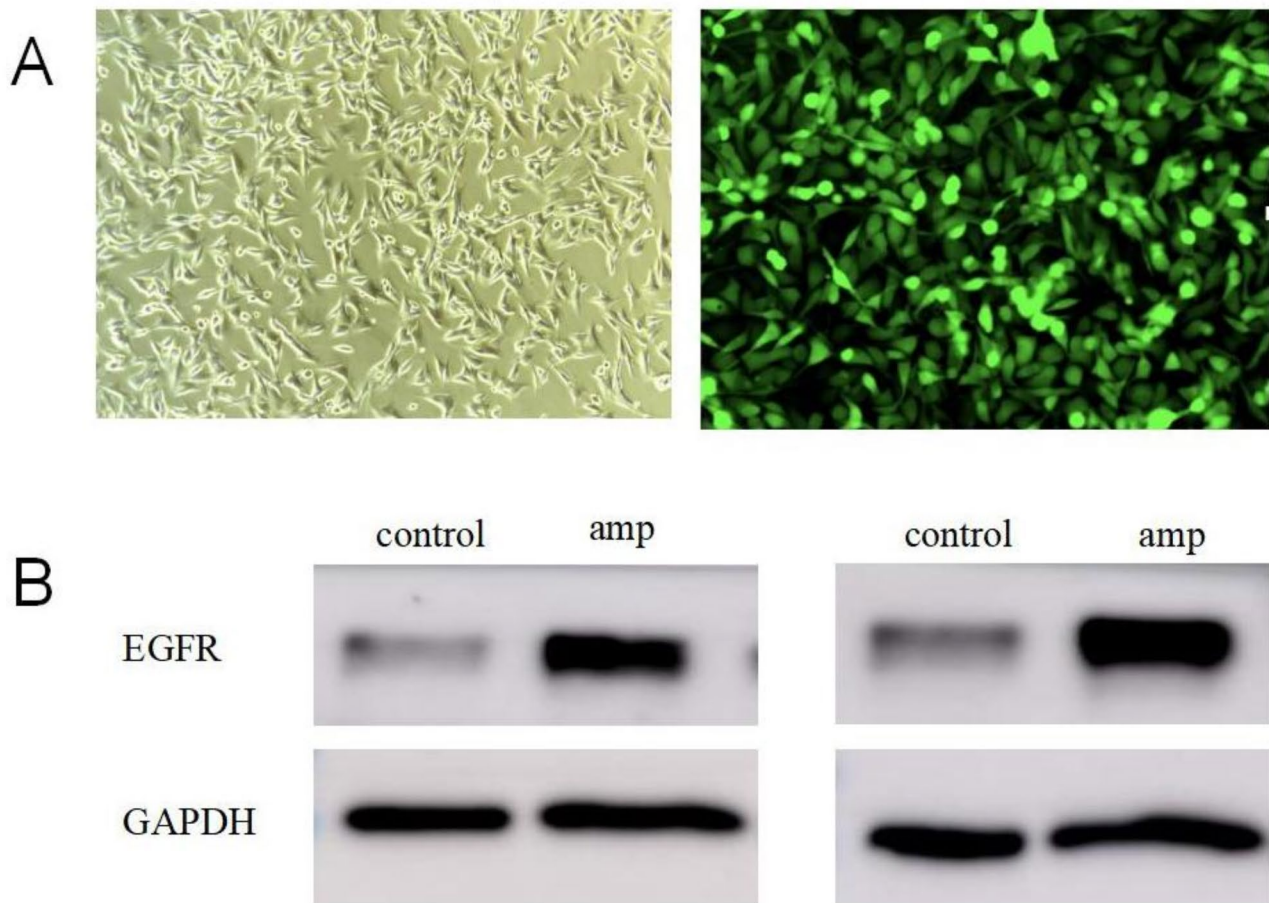


Fig. 4 Images from the light microscope showed that the PC9 cell line (A) was successfully transfected by EGFR-overexpressing lentivirus. Western blot showed that the expression of EGFR proteins was successfully increased in PC9 cell lines (B) due to Lentivirus transduction

In our study, we found that *EGFR* overexpression enhances cell proliferation and migration. In vivo experiments further demonstrated that, compared to the control group, animals with high *EGFR* expression exhibited a significantly higher incidence of brain metastases. Sequencing data suggested that the negative regulation of cell adhesion might be a key factor promoting brain metastasis. However, our study has several limitations. First, the biological validation of *LGALS1*, the gene we identified through differential analysis, is still in its early stages and requires further investigation. Second, the mechanistic link between *EGFR* and the negative regulation of cell adhesion in contributing to brain metastasis

remains unclear, as does the interplay between *EGFR* and *LGALS1* and the downstream pathways involved. These aspects warrant further exploration in future studies. Current therapies are mainly palliative and do not improve survival for most patients and advances in several therapeutic modalities have effectively challenged the lethal nature of brain metastasis for specific subsets of patients [19]. Our results suggest that overexpression of the *EGFR* gene may play an important role in the process of brain metastasis in lung cancer patients. Interventions targeting this gene could potentially offer new treatment options for lung cancer patients with metastasis to the brain.

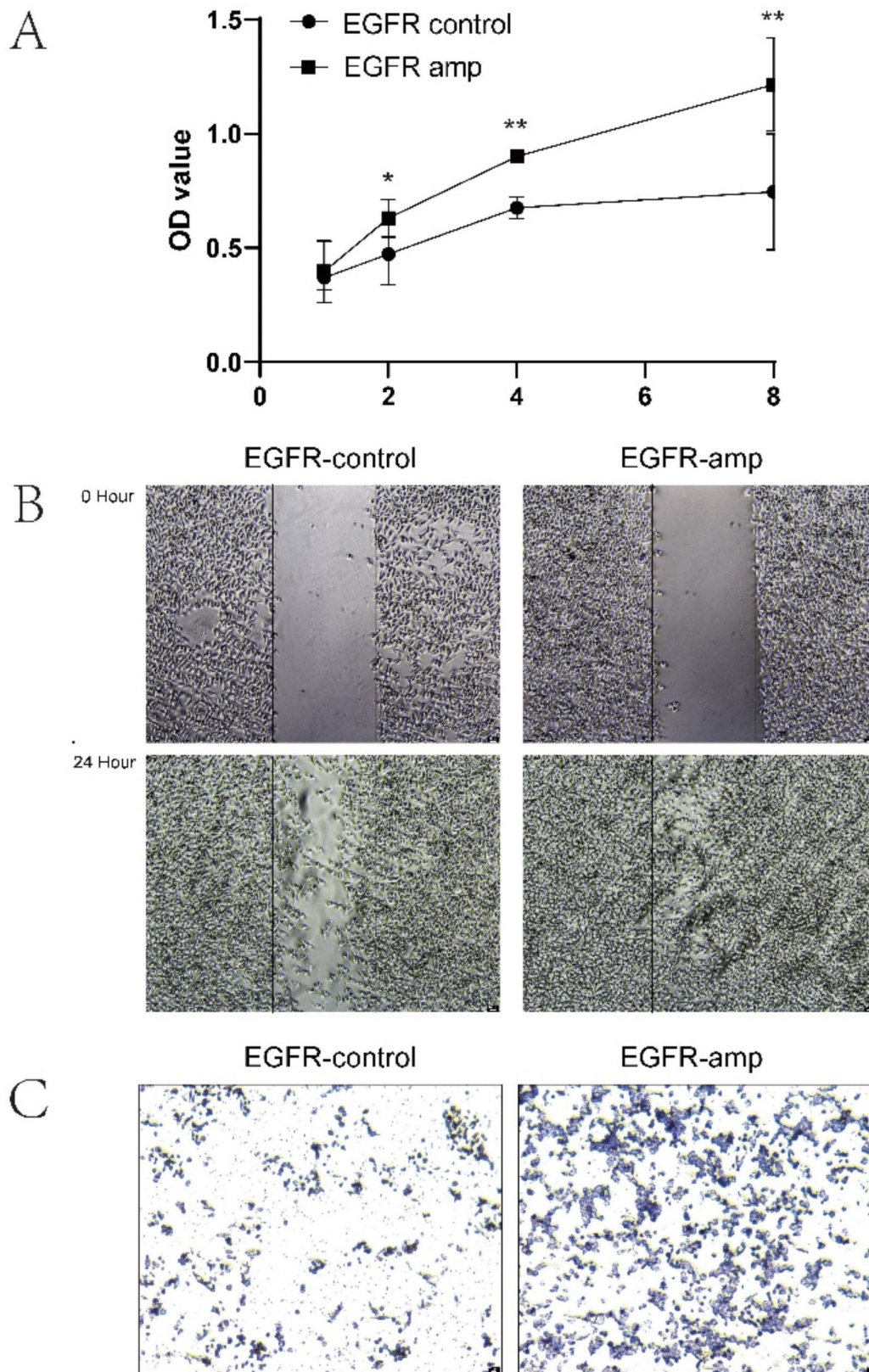


Fig. 5 Proliferation and migration ability of NSCLC cell lines in vitro. **(A)** CCK8 test was performed to assess the proliferation ability of PC9 cell line, Data are represented as means \pm SD. **(B)** wound healing was performed to assess the migration ability of PC9 cell line. **(C)** Transwell assays was performed to assess the infiltration ability of PC9 cell line

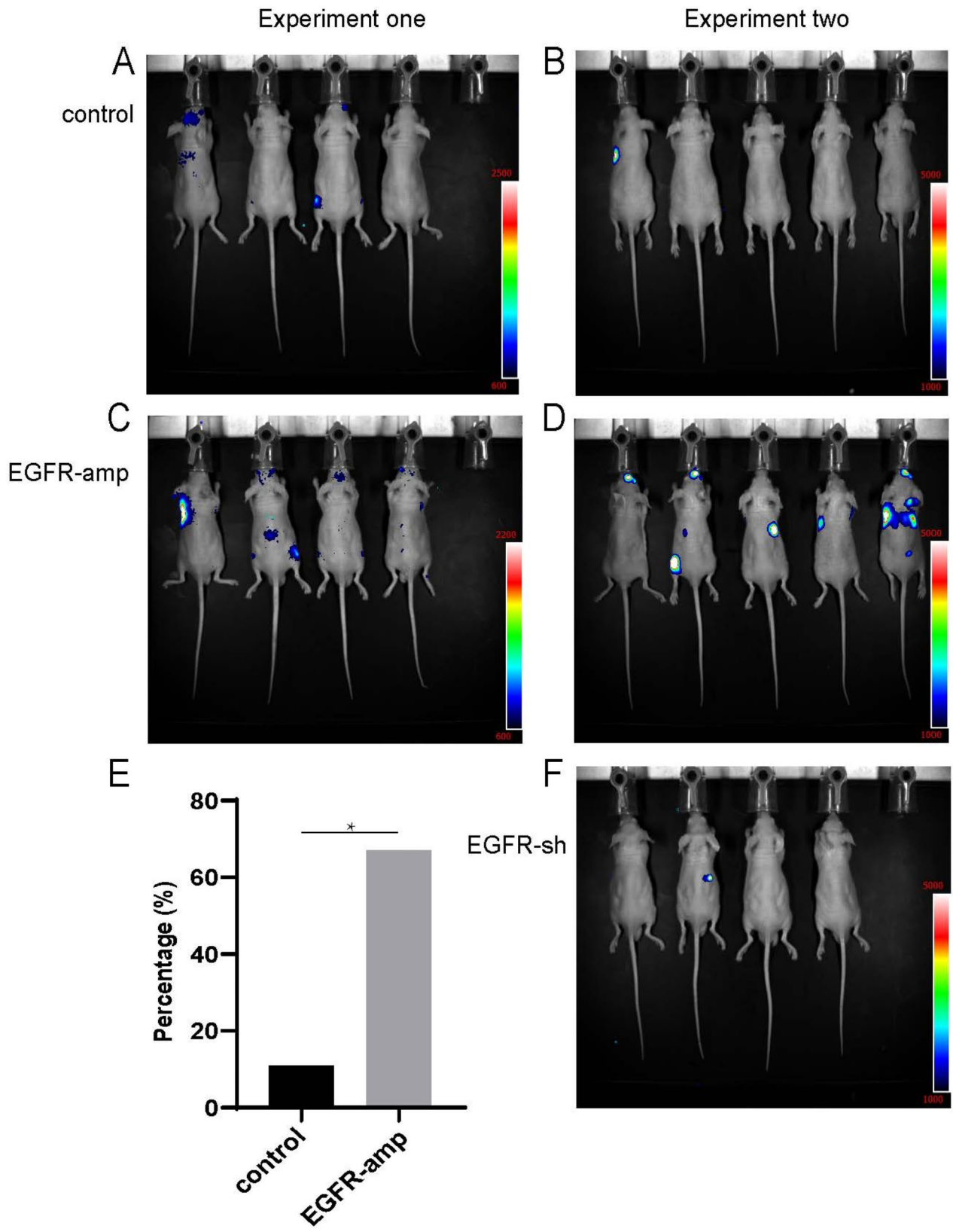


Fig. 6 Figure A-B presents the distribution of brain metastases in the control group. C-D presents the distribution of brain metastases in overexpression of the EGFR protein group (EGFR-amp). E shows the brain metastasis rate between EGFR-amp and the control group. F shows the distribution of brain metastases in the loss of function of EGFR protein group (EGFR-sh)

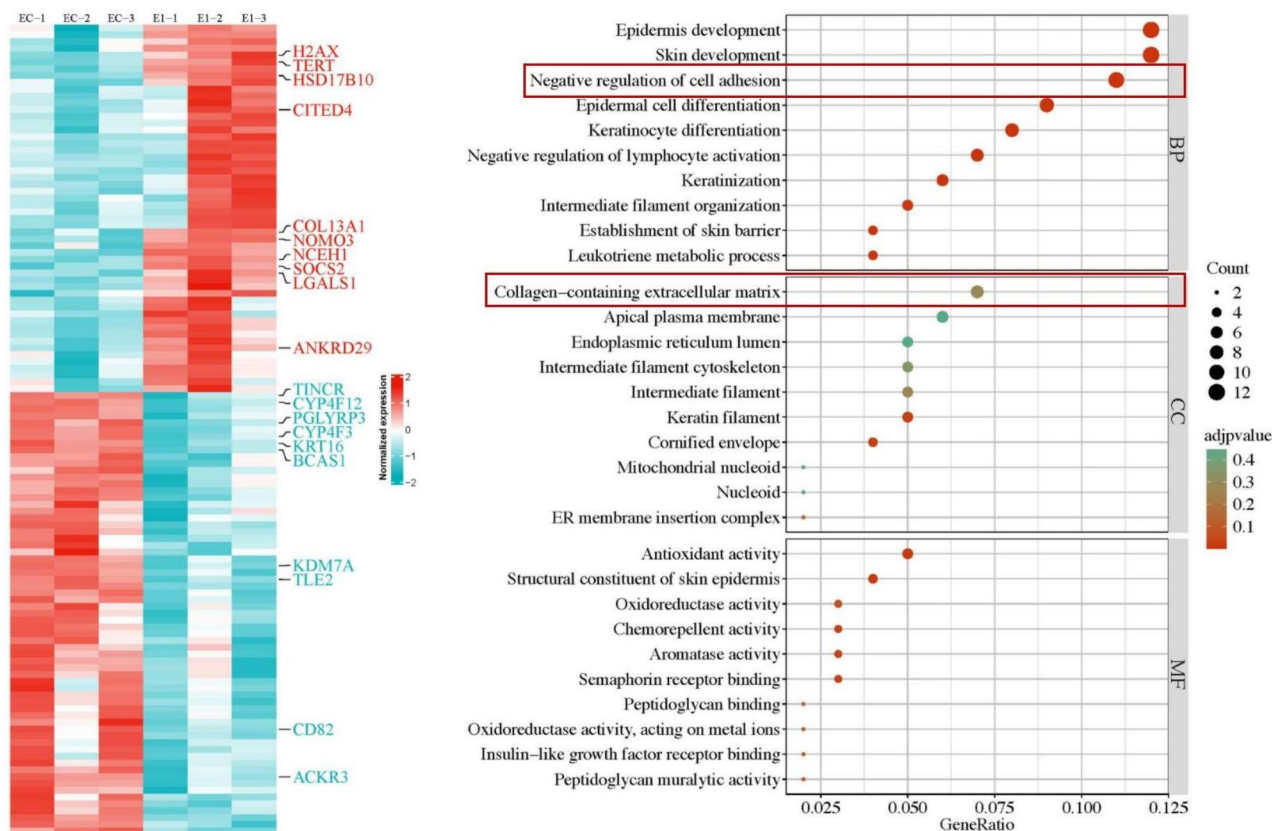


Fig. 7 Heatmap of differentially expressed genes between EGFR-amp versus control group (Left). Bubble chart plotted against the results of GO analysis for the differential expression (Right)

Supplementary Information

The online version contains supplementary material available at <https://doi.org/10.1186/s12575-025-00277-2>.

Supplementary Material 1: Supplementary Data Fig. 1 Tumor cells were injected subcutaneously in the experiment mice and growth curves was plotted. Supplementary Data Fig. 2-3 H&E stained images of resected mouse subcutaneous tumors.

Acknowledgements

Not applicable.

Author Contributions

Hainan Yang, Congli Hu, Yu Zhou, designed the experiments and wrote the manuscript. Taoyuan Tong, luyao Qi, Yuan Weifang, helped in reviewing, acquisition, analysis and interpretation of clinical data for the work. Changguo Shan, Weiping Hong did the statistical analysis. Wen Lei, Caicun Zhou, Ming Lei revised critically the manuscript for important intellectual content. All authors have read and approved the final manuscript.

Funding

This study is funded by The Scientific Research Program of Shanghai Pudong New Area Health Commission (the General Program, Grant No.PW2024A-58), National Natural Science Foundation of China (82174189, 82304920), Discipline Development Program of the Shanghai Pudong New Area Health Commission (PWxq2022-09).

Data Availability

No datasets were generated or analysed during the current study.

Declarations

Ethics Approval and Consent to Participate

This study was conducted in accordance with the Declaration of Helsinki and approved by the Ethics Committee of Guangdong Sanjiu Brain Hospital. We informed the participants about the study and obtained informed consent from each patient.

Consent for Publication

Written informed consent was obtained from all patients for the study.

Competing Interests

The authors declare no competing interests.

Author details

- ¹Department of Critical Care Medicine, Seventh People’s Hospital of Shanghai University of Traditional Chinese Medicine, 358 Datong Road, Pudong New District, Shanghai 200137, China
- ²Department of Oncology, School of Medicine, Shanghai Pulmonary Hospital & Thoracic Cancer Institute, Tongji University, Shanghai 200092, China
- ³Department of Medical Genetics, School of Medicine, Tongji University, Shanghai 200092, China
- ⁴School of Life Sciences and Technology, Tongji University, Shanghai 200092, China
- ⁵Department of Oncology, Guangdong Sanjiu Brain Hospital, Guangzhou, China
- ⁶Department of Radiation Oncology, Zhujiang Hospital, Southern Medical University, 253 Gongye Dadao, Guangzhou, Guangdong 510280, China
- ⁷Department of Medical Oncology, School of Medicine, Shanghai Pulmonary Hospital & Thoracic Cancer Institute, Tongji University, No. 507, Zheng Min Road, Shanghai 200433, China

Received: 19 January 2025 / Accepted: 2 April 2025

Published online: 23 April 2025

References

1. Barnholtz-Sloan JS, Sloan AE, Davis FG, Vignea FD, Lai P, Sawaya RE. Incidence proportions of brain metastases in patients diagnosed (1973 to 2001) in the metropolitan Detroit cancer surveillance system. *J Clin Oncol*. 2004;22(14):2865–72.
2. Consonni D, Pierobon M, Gail MH, Rubagotti M, Rotunno M, Goldstein A, et al. Lung cancer prognosis before and after recurrence in a population-based setting. *J Natl Cancer Inst*. 2015;107(6):dju059.
3. Cagney DN, Martin AM, Catalano PJ, Redig AJ, Lin NU, Lee EQ, et al. Incidence and prognosis of patients with brain metastases at diagnosis of systemic malignancy: a population-based study. *Neuro Oncol*. 2017;19(11):1511–21.
4. Rybarczyk-Kasiuchnicz A, Ramlau R, Stencel K. Treatment of brain metastases of non-small cell lung carcinoma. *Int J Mol Sci*. 2021;22(2).
5. Zabel A, Debus J. Treatment of brain metastases from non-small-cell lung cancer (NSCLC): radiotherapy. *Lung Cancer*. 2004;45(Suppl 2):S247–52.
6. Shah N, Liu Z, Tallman RM, Mohammad A, Sprowls SA, Saralkar PA, et al. Drug resist occurred new characterized preclinical model lung cancer brain metastasis. *BMC Cancer*. 2020;20(1):292.
7. Gril B, Palmieri D, Bronder JL, Herring JM, Vega-Valle E, Feigenbaum L, et al. Effect of lapatinib on the outgrowth of metastatic breast cancer cells to the brain. *J Natl Cancer Inst*. 2008;100(15):1092–103.
8. Gállego Pérez-Larraya J, Hildebrand J. Brain metastases. *Handb Clin Neurol*. 2014;121:1143–57.
9. Guérin A, Sasane M, Dea K, Zhang J, Culver K, Nitulescu R, Wu EQ, Macalalad AR. The economic burden of brain metastasis among lung cancer patients in the united States. *J Med Econ*. 2016;19(5):526–36.
10. Schouten LJ, Rutten J, Huvneers HA, Twijnstra A. Incidence of brain metastases in a cohort of patients with carcinoma of the breast, colon, kidney, and lung and melanoma. *Cancer*. 2002;94(10):2698–705.
11. Costa V, Kowalski LP, Coutinho-Camillo CM, Begnami MD, Calsavara VF, Neves JI, Kaminagakura E. EGFR amplification and expression in oral squamous cell carcinoma in young adults. *Int J Oral Maxillofac Surg*. 2018;47(7):817–23.
12. Xia W, Lau YK, Zhang HZ, Xiao FY, Johnston DA, Liu AR, Li L, Katz RL, Hung MC. Combination of EGFR, HER-2/neu, and HER-3 is a stronger predictor for the outcome of oral squamous cell carcinoma than any individual family members. *Clin Cancer Res*. 1999;5(12):4164–74.
13. Szabó B, Nelhubel GA, Kárpáti A, Kenessey I, Jóri B, Székely C et al. Clinical significance of genetic alterations and expression of epidermal growth factor receptor (EGFR) in head and neck squamous cell carcinomas. *Oral Oncol*. 2011;47(6):487–96.
14. Huang SF, Cheng SD, Chien HT, Liao CT, Chen IH, Wang HM, Chuang WY, Wang CY, Hsieh LL. Relationship between epidermal growth factor receptor gene copy number and protein expression in oral cavity squamous cell carcinoma. *Oral Oncol*. 2012;48(1):67–72.
15. Zhou W, Liu Z, Wang Y, Zhang Y, Qian F, Lu J et al. The clinicopathological and molecular characteristics of resected EGFR-mutant lung adenocarcinoma. *Cancer Med*. 2022;11(5):1299–309.
16. Xu J, Li P, Wang Y, Li J, Xu B, Zhao J, et al. The role of proliferating stem-like plasma cells in relapsed or refractory multiple myeloma: insights from single-cell RNA sequencing and proteomic analysis. *Br J Haematol*. 2024;205(3):1031–43.
17. Zhou L, Tian J, Wang K, Ma Y, Chen X, Luo H et al. Targeting Galectin-1 overcomes Paclitaxel resistance in esophageal squamous cell carcinoma. *Cancer Res*. 2024;84(22):3894–908.
18. Yang F, Li T, Zhang XQ, Gong Y, Su H, Fan J, Wang L, Hu QD, Tan RZ. Screening of active components in astragalus mongholicus bunge and Panax Notoginseng formula for anti-fibrosis in CKD: nobiletin inhibits Lgals1/PI3K/AKT signaling to improve renal fibrosis. *Ren Fail*. 2024;46(2):2375033.
19. Peters S, Camidge DR, Shaw AT, Gadgeel S, Ahn JS, Kim DW et al. Alectinib versus Crizotinib in untreated ALK-positive non-small-cell lung cancer. *N Engl J Med*. 2017;377(9):829–38.

Publisher's Note

Springer Nature remains neutral with regard to jurisdictional claims in published maps and institutional affiliations.